Parra et al. Nanoscale Research Letters (2018) 13:40
DOI 10.1186/s11671-018-2449-x

Nanoscale Research Letters

NANO EXPRESS Open Access

Stimulation of Cysteine-Coated CdSe/ZnS Quantum Dot Luminescence by *meso*-Tetrakis (p-sulfonato-phenyl) Porphyrin

Gustavo G. Parra[1,5*], Lucimara P. Ferreira[1], Pablo J. Gonçalves[2], Svetlana V. Sizova[3], Vladimir A. Oleinikov[3], Vladimir N. Morozov[4], Vladimir A. Kuzmin[4] and Iouri E. Borissevitch[1,2]

Abstract

Interaction between porphyrins and quantum dots (QD) via energy and/or charge transfer is usually accompanied by reduction of the QD luminescence intensity and lifetime. However, for CdSe/ZnS-Cys QD water solutions, kept at 276 K during 3 months (aged QD), the significant increase in the luminescence intensity at the addition of *meso*-tetrakis (p-sulfonato-phenyl) porphyrin ($TPPS_4$) has been observed in this study. Aggregation of QD during the storage provokes reduction in the quantum yield and lifetime of their luminescence. Using steady-state and time-resolved fluorescence techniques, we demonstrated that $TPPS_4$ stimulated disaggregation of aged CdSe/ZnS-Cys QD in aqueous solutions, increasing the quantum yield of their luminescence, which finally reached that of the fresh-prepared QD. Disaggregation takes place due to increase in electrostatic repulsion between QD at their binding with negatively charged porphyrin molecules. Binding of just four porphyrin molecules per single QD was sufficient for total QD disaggregation. The analysis of QD luminescence decay curves demonstrated that disaggregation stronger affected the luminescence related with the electron-hole annihilation in the QD shell. The obtained results demonstrate the way to repair aged QD by adding of some molecules or ions to the solutions, stimulating QD disaggregation and restoring their luminescence characteristics, which could be important for QD biomedical applications, such as bioimaging and fluorescence diagnostics. On the other hand, the disaggregation is important for QD applications in biology and medicine since it reduces the size of the particles facilitating their internalization into living cells across the cell membrane.

Keywords: Luminescence stimulation, Cysteine-coated quantum dot, $TPPS_4$ porphyrin, Disaggregation, Electrostatic interaction

Background

Colloidal semiconductor nanocrystals or quantum dots (QD) due to their specific characteristics, intense broad absorption and narrow luminescence spectra with the size-dependent maximum position and high thermal and photostability [1, 2], find applications in various fields of modern technology, such as medical imaging and diagnostics, modern computing nanodevices, fluorescent probes for bioanalytical applications, photoelectrochemical hydrogen generation, etc. ([3–7] and references therein). Functionalization of the QD surface with organic molecules makes it possible to increase their solubility in water, to reduce their toxicity, and to increase their biocompatibility, preparing QD with selective affinity to desirable structures of living organisms [8]. Therefore, QD attract special interest for applications in biology [5] and medicine [6], where they could be successfully applied as fluorescent probes (FP) for fluorescence diagnostics (FD) [9] and photosensitizers (PS) for photochemotherapy (PCT) [10]. Intense absorption in a broad spectral region makes QD an effective antenna for light energy accumulation, and intense narrow luminescence band facilitates the energy transfer to corresponding PS, thus increasing the efficiency of the light energy utilization and consequently increasing the PS efficacy

* Correspondence: gugparra@gmail.com
[1]Departamento de Física, Faculdade de Filosofia, Ciências e Letras de Ribeirão Preto, Universidade de São Paulo, Ribeirão Preto, SP 14040-901, Brazil
[5]Present Address: MackGraphe, Mackenzie Presbyterian University, São Paulo, SP 01302-907, Brazil
Full list of author information is available at the end of the article

[7, 11]. This makes (QD+PS) pairs promising for application in FD and PCT and stimulates studies in the QD and FS interaction, especially in the transfer of energy and charge between them.

Among others, cysteine-coated (CdSe/ZnS) QD ((CdSe/ZnS)-Cys QD) and *meso*-tetrakis (p-sulfonato-phenyl) porphyrin ($TPPS_4$) attract a special interest due to following reasons: a small size of cysteine-coated QD (QD-Cys) which increases its mobility and the probability to penetrate cell membrane, its high chemical stability, low nonspecific adsorption, and high luminescence quantum yield [12, 13]. On the other hand, synthetic $TPPS_4$ porphyrin is a promising PS since it is photoactive, water soluble, and non-toxic and has already been tested in clinics in application in photodynamic therapy (PDT) demonstrating hopeful characteristics [14, 15].

Interaction between $TPPS_4$ and QD via energy and/or charge transfer has already been documented [16]. Commonly, these processes are accompanied by reduction in the QD luminescence intensity and lifetime. One more process that causes luminescence self-quenching in QD is the self-aggregation via electrostatic interactions or hydrogen bond formation, in many cases, making the aggregation process reversible [17].

In this work, we report for the first time on the stimulation of the QD luminescence via interaction with porphyrin on the example of (CdSe/ZnS)-Cys QD and $TPPS_4$ porphyrin.

Experimental

Preparation of (CdSe/ZnS)-Cys Quantum Dots

The (CdSe/ZnS)-Cys QD were synthesized in accordance with the method adapted from [18]. The method includes the following: (1) synthesis of colloidal hydrophobic CdSe core nanocrystals and (2) growth of an epitaxial ZnS shell around the CdSe core. To functionalize QD with cysteine, the resultant CdSe/ZnS core–shell QD (~ 3.0 mg) were purified from TOPO via threefold dispersing in chloroform (500 mL) and precipitating with methanol (800 mL). Purified QD were re-dispersed in chloroform (1.0 mL). DL-Cysteine in methanol (30 mg mL^{-1}, 200 mL) was added dropwise to the QD dispersion and mixed vigorously followed by centrifugation (10,000 rpm, 5 min), removing chloroform. After washing with methanol to remove the excess of DL-Cysteine through centrifugation (16,000 rpm, 10 min, 3 times), the QD precipitate was dried under vacuum and re-dispersed in Milli-Q water with 1 M NaOH (20 mL) dropwise addition and filtered with syringe filter Anotop 25 Plus (0.02 μm, Whatman).

Preparation of porphyrin + (CdSe/ZnS)-Cys QD Samples

The $TPPS_4$ porphyrin was obtained from Midcentury Chemicals (USA) and used without additional purification. The experimental solutions were prepared in phosphate buffer (pH 7.3; 7.5 mM), using Milli-Q quality water. For luminescence measurements in (CdSe/ZnS)-Cys QD kept at 276 K for 3 months (aged QD), aliquots of a concentrated $TPPS_4$ stock solution ($[TPPS_4]_{stock}$ = 140 μM) were added to the (CdSe/ZnS)-Cys QD initial solution, avoiding dilution effects. For the aged QD dilution experiment, aliquots of the initial solution were replaced by the same amount of phosphate buffer. All the experiments were performed at room temperature (297 K).

The concentration of $TPPS_4$ was controlled spectrophotometrically using $\varepsilon_{515nm} = 1.3 \times 10^4\ M^{-1}\ cm^{-1}$ [19]. The concentration of the aged (CdSe/ZnS)-Cys quantum dot was calculated using the first excitonic absorption peak at 520 nm using $\varepsilon = 5857(D)^{2.65}$ according to Yu's empirical calculation [20], where D(nm) is the diameter of the given nanocrystal. The D value was determined from the empirical fitting function of the curve as presented in [20]. For CdSe nanocrystals, this function is:

$$D = \left(1.6122 \times 10^{-9}\right)\lambda^4 - \left(2.6575 \times 10^{-6}\right)\lambda^3 + \left(1.6242 \times 10^{-3}\right)\lambda^2 - (0.4277)\lambda + (41.57) \quad (1)$$

In our case, $\lambda = 520$ nm, $D = 2.6$ nm, and $\varepsilon = 7.4 \times 10^4\ M^{-1}\ cm^{-1}$.

Instruments

The absorption spectra were monitored with a Beckman Coulter DU640 spectrophotometer. The steady-state luminescence measurements were made on a Hitachi F-7000 spectrofluorimeter at $\lambda_{ex} = 480$ nm and $\lambda_{em} = 558$ nm. The aged QD luminescence quantum yield (QY) was determined via relative method [21] with a single point measurement, $\lambda_{ex} = 480$ nm and $\lambda_{em} = 558$ nm, using 1-palmitoyl,2-(12-[N-(7-nitrobenz-2-oxa-1,3-diazol-4-yl)amino]dodecanoyl)-sn-glycero-3-phospho choline (C12-NBD-PC) as a standard (QY = 0.34 in ethanol) [22, 23] according to the equation:

$$\Phi_{fl} = \Phi_{fl0}\frac{n^2 I_{fl}}{n_0^2 I_{fl0}}\frac{A_0}{A} \quad (2)$$

where I_{fl} and I_{fl0} are the integral fluorescence intensities of QD and C12-NBD-PC, A and A_0 are their absorbances at $\lambda_{ex} = 480$ nm, and n and n_0 are refractive indexes of the used solvents, respectively.

Time-resolved experiments were carried out by using an apparatus based on the time-correlated single-photon counting method. The excitation source was a Tsunami 3950 Spectra Physics titanium-sapphire laser, pumped by a Millenia X Spectra Physics solid state laser. The frequency of the laser pulse repetition was 8.0 MHz using the 3980 Spectra Physics pulse picker. The laser was tuned so that the second harmonic generator BBO

crystal (GWN-23PL Spectra Physics) gave the 480 nm excitation pulses that were directed to an Edinburgh FL900 spectrometer. The spectrometer was in L-format configuration, the emission wavelength was selected by a monochromator, and the emitted photons were detected by a refrigerated Hamamatsu R3809U microchannel plate photomultiplier. The full width at half maximum (FWHM) of the instrument response function was typically 100 ps, and time resolution was 12 ps per channel. The software provided by Edinburgh Instruments and the commercial "OriginPro9" software were used to fit the experimental luminescence decay curves.

The quality of the fit was evaluated by the analysis of the statistical parameter reduced-χ^2 and by inspection of the residuals distribution.

Dynamic light scattering was measured with Nano-Brook 90Plus Zeta Particle Size Analyzer with excitation at 640 nm using a 40 mW HeNe laser (Brookhaven Instruments Corporation).

Results and Discussion

Freshly prepared (CdSe/ZnS)-Cys QD possess the maximum of the luminescence spectrum at 558 nm (Fig. 1, black line), as previously reported by Liu et al. [13], and quantum yield (QY) 0.75 [2, 24, 25]. The addition of $TPPS_4$ to the fresh solution induces no changes, both in the QD luminescence intensity and the luminescence spectrum profile.

For (CdSe/ZnS)-Cys QD dissolved in water and kept in the refrigerator at 276 K for 3 months (aged QD), the position of the maximum of the luminescence spectrum, measured in phosphate buffer (7.5 mM) at pH 7.3, was blue-shifted for 2 nm (λ_{max} = 556 nm), as compared with

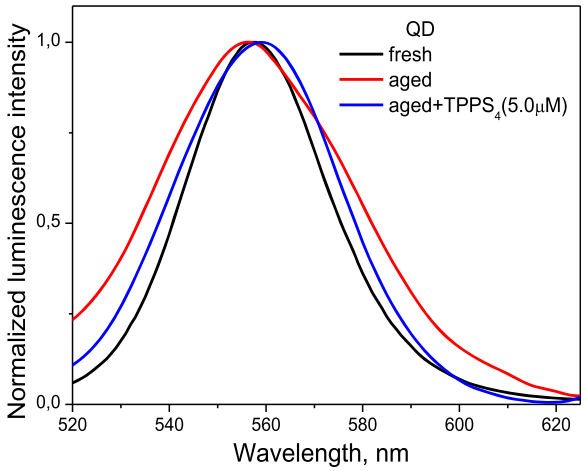

Fig. 1 Normalized luminescence spectra of (CdSe/ZnS)-Cys 558 quantum dots in phosphate buffer (7.5 mM) at pH 7.3: fresh prepared (black line, λ_{max} = 558 nm), after 3 months in the refrigerator at 276 K (aged QD) without $TPPS_4$ (red line, λ_{max} = 556 nm), and at addition of [$TPPS_4$] = 5.0 μM to aged QD (blue line, λ_{max} = 559 nm), λ_{ex} = 480 nm

that of fresh QD. The emission band appeared widened and slightly asymmetric (Fig. 1, red line). The quantum yield of the aged QD luminescence, determined by the method described above, was 0.23 ± 0.03.

The addition of $TPPS_4$ to the aged QD solution induced significant increase in the luminescence intensity (Fig. 2a), QY value reaching 0.75 ± 0.08 (Fig. 2a, inset), the value closed to that for fresh QD [2, 24, 25].

Moreover, in the presence of $TPPS_4$, the symmetrization of the luminescence band of the aged QD and the reduction of its bandwidth were observed, accompanied by maximum red shift up to λ_{max} = 559 nm, close to the maximum of the fresh QD spectrum (Fig. 1, blue line.).

The luminescence decay curves obtained at 480 nm excitation for solutions of both fresh and aged QD were successively fitted as a sum of three exponentials:

$$I = I_{0_1} e^{-t/\tau_1} + I_{0_2} e^{-t/\tau_2} + I_{0_3} e^{-t/\tau_3} \quad (3)$$

where I_{0_i} and τ_i are pre-exponential factor (amplitude) and lifetime of the i-th decay component, respectively.

The component lifetimes for both fresh and aged QD are independent from the porphyrin presence (Table 1). The luminescence lifetimes of fresh QD solutions are typical for (CdSe/ZnS)-Cys QD [26, 27]. For aged QD, the component lifetimes are much shorter (Table 1).

The values of τ_1 in all cases, fresh and aged QD in the presence and absence of porphyrin, are close to time resolution of the single-photon counting equipment (≈ 100 ps) used in this study. Therefore, it should be associated with the scattered light of the exciting pulse.

It is well established [28–30] that the short-lived (τ_2) and long-lived (τ_3) components are associated with the luminescence resulted from the electron-hole annihilation in the QD core (τ_2) and shell (τ_3), respectively. Total intensity of these two components characterizes the whole annihilation process in the QD. In this case, the relative intensity (amplitude) of the τ_3 component should demonstrate the contribution of the electron-hole annihilation in the QD shell. The relative contribution I_3 of 3rd component to the decay curve was calculated as:

$$I_3 = \frac{I_{0_3}}{I_{0_2} + I_{0_3}} \quad (4)$$

The addition of $TPPS_4$ to fresh QD solutions does not change significantly the relative content of the components (data not shown), while for aged QD solutions, the relative content of τ_3 component I_3 increases with the $TPPS_4$ concentration (Fig. 2b, inset). The dependence of QY for aged quantum dot luminescence on the $TPPS_4$ concentration is similar to that for I_3 (Fig. 2a, b, insets), both reaching the maximum values approximately at 2.0 μM $TPPS_4$. This means that $TPPS_4$ interacting with

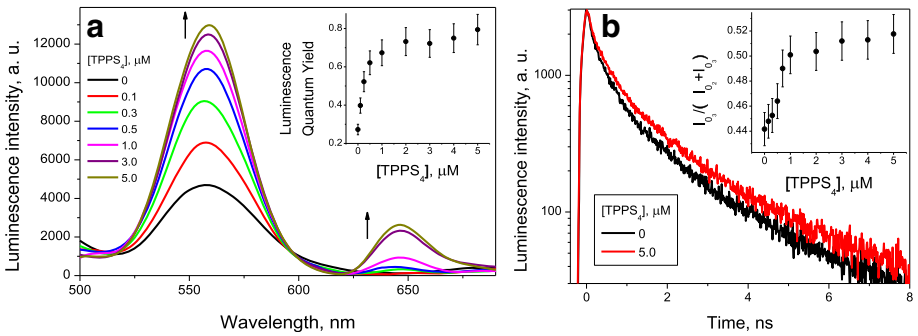

Fig. 2 **a** Luminescence spectra and quantum yield (inset) of aged (CdSe/ZnS)-Cys 558 QD ([QD] = 570 nM, black curve) solutions as a function of the $TPPS_4$ porphyrin concentration. **b** Decay kinetics of QD luminescence and the $I_{03}/(I_{02}+I_{03})$ ratio (inset, see Eq. (3)) as a function of the $TPPS_4$ porphyrin concentration

aged QD affects stronger the luminescence of QD shell than that of its core. However, $TPPS_4$ in fresh QD solutions demonstrates no effect upon the QD luminescence. Therefore, we conclude that the $TPPS_4$ effect observed for the aged QD solution cannot be explained by the porphyrin binding to the QD surface.

On the other hand, the observed increase of the aged QD luminescence intensity at interaction with $TPPS_4$ cannot be explained via reverse energy transfer from $TPPS_4$ to QD, since the $TPPS_4$ fluorescence spectrum is localized in the range $\lambda > 600$ nm where QD absorption is weak (Additional file 1: Figure S3). Therefore, the energy transfer via Förster resonance energy transfer (FRET) mechanism is low probable. Moreover, the QD luminescence was excited at 460 or 480 nm, where $TPPS_4$ optical absorption is negligible. In addition, the absorption spectra of $TPPS_4$ remained unchanged in the mixed solutions, demonstrating the absence of charge transfer between QD and $TPPS_4$ (Additional file 1: Figure S4b, c).

The ability of quantum dots to aggregate via formation of non-covalent NH···H hydrogen bonds between the QD surface groups was already documented [13, 17]. Aggregation reduces the QD luminescence, quenching most effectively the component attributed to the QD shell [13, 17]. The reduction of the QD luminescence intensity and lifetime was observed for CdSe-QD in solid films due to formation of 3D aggregates [31]. The authors proposed a model, where this reduction is associated with energy transfer between individual QD in the aggregate [32].

Table 1 Lifetimes of the (CdSe/ZnS)-Cys QD luminescence decay curve components in phosphate buffer (7.5 mM) at pH 7.3: fresh QD and those after 3 months in the refrigerator at 276 K (aged QD) in the absence and presence of $TPPS_4$, $\lambda_{ex} = 480$ nm, $\lambda_{em} = 558$ nm

Sample	τ_1, ns	τ_2, ns	τ_3, ns
Fresh QD	0.7 ± 0.1	3.8 ± 0.4	19 ± 1
Fresh QD + 8.6μM [$TPPS_4$]	0.7 ± 0.1	4.1 ± 0.5	20 ± 1
Aged QD	0.1 ± 0.1	1.0 ± 0.2	5.2 ± 0.5
Aged QD + 5.0μM [$TPPS_4$]	0.1 ± 0.1	0.9 ± 0.2	5.2 ± 0.5

On the bases of this evidence, we believe that while in the refrigerator, QD do aggregate, which reduces the luminescence intensity and lifetimes. Therefore, we associate the observed increase in the QD luminescence intensity and lifetimes in the presence of $TPPS_4$ with QD disaggregation, stimulated by $TPPS_4$ at its binding with the aggregate. The similar effect was observed for the emission of aggregated QD at their interaction with fluorine ions [17].

The observed changes in the luminescence band profile for aged QD (Fig. 1) can be explained by QD aggregation, as well, its asymmetry being associated with existence of different types of aggregates. Interaction with $TPPS_4$ reduces aggregation and makes the luminescence band profile similar to that for non-aggregated QD, observed in fresh solutions.

At neutral pH, the QD-Cys surface possesses negative net charge due to deprotonation of terminal amino groups on its surface [17, 33, 34]. At this pH, $TPPS_4$ has net charge (4-) due to four negatively charged sulfonate phenyl groups in its structure ([35, 36] and references therein). Therefore, interaction between QD cysteine groups and $TPPS_4$ molecules is low probable because of electrostatic repulsion. However, high affinity of the porphyrin π-conjugated system for metal surfaces is well documented [37]. This affinity should be responsible for $TPPS_4$ binding on the quantum dots surface, despite of the electrostatic repulsion between the QD and porphyrin side groups. The interaction between QD surface and π-conjugated system of the bound porphyrin could explain weak broadening of the porphyrin fluorescence spectrum (Figs. 1, 3, and Additional file 1: Figure S3a, inset) and observed changes in the fluorescence excitation spectrum (Additional file 1: Figure S5b, inset) [38].

Binding of some porphyrin molecules on the QD surface increases the QD surface negative charge, thus

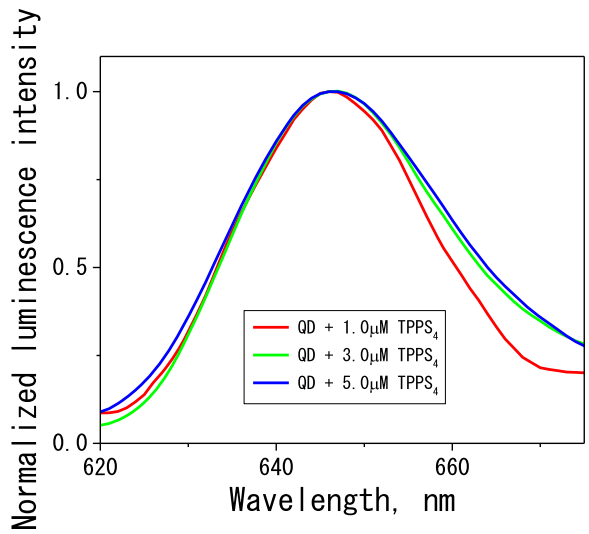

Fig. 3 Normalized luminescence emission spectra of $TPPS_4$ in phosphate buffer (7.5 mM, pH 7.3) for various $TPPS_4$ concentrations in the presence of aged (CdSe/ZnS)-Cys 558 quantum dot (570 nM), $\lambda_{ex} = 460$ nm

increasing electrostatic repulsion between particles and inducing their disaggregation (Scheme 1) [39].

The QD surface area $A_{QD} \approx 145$ nm^2 is sufficient to adsorb several $TPPS_4$ molecules ($A_{TPPS4} \approx 1.8$ nm^2 per unit) [40], as it was observed for porphyrins interacting with magnetic and gold nanoparticles [41, 42].

To cover the whole area of QD by porphyrins, 80 porphyrin molecules per individual QD are necessary. However, the saturation of the luminescence QY and I_3 values in 570 nM QD solution was observed at approximately $[TPPS_4] = 2.0$ μM (Fig. 2), which demonstrates that the binding of four porphyrin molecules per QD is sufficient for QD disaggregation. This could be explained by larger charge density on the porphyrin molecule as compared with that of QD (Additional file 1: Figure S6) which produces stronger electrostatic repulsion between QD with bound porphyrins. Indeed, Zeta-potential for the aged QD (ζ_{QD}) is − 36.1 mV and that for $TPPS_4$ molecule (ζ_{TPPS4}) is − 37.6 mV. Average charge density, calculated as $\sigma = \zeta / A_{QD}$, for an individual aged QD is

$\sigma_{QD} = -36.1$ mV/145 nm^2 = − 0.25 mV/nm^2.

At the same time, for an individual aged QD bound with four $TPPS_4$ molecules, the average charge density ($\sigma_{QD+TPPS4}$) is

$\sigma_{QD+TPPS4} = -(36.1 + 37.6 \times 4)$ mV/145 nm^2 = − 1.29 mV/nm^2.

Thus, the binding of four $TPPS_4$ molecules with an individual aged QD increases its σ more than 5 times, increasing the force of electrostatic repulsion more than 25 times and inducing the aged QD disaggregation.

In accordance with the QD aggregation hypothesis, a similar effect to that induced by $TPPS_4$ addition should be observed at dilution of aged QD solutions. Really, we have observed the increase in the QY of QD luminescence at dilution of its buffer solution (Fig. 4a, inset), which demonstrates that the self-quenching of QD luminescence in aged QD-Cys solutions depends on QD concentration [17]. Simultaneously, the I_3 value in the QD luminescence kinetics increases with dilution, as well (Fig. 4b, inset).

Moreover, the dynamic light scattering experiments show that D_{hd} of scattering particles in the QD solutions after aging was (330 ± 170) nm, which is much larger than that of fresh QD. Dilution reduces D_{hd} down to (25 ± 6) nm, thus demonstrating directly the QD disaggregation (Additional file 1: Table S1).

There exists one more interesting aspect of the problem: can addition of $TPPS_4$ to the solution of fresh QD prevent their aggregation during storage at low temperature, thus stabilizing their luminescence characteristics? However, clarification of this problem needs an independent and detailed study using various experimental methods and varying experimental conditions, such as reagent concentrations, temperature, duration of

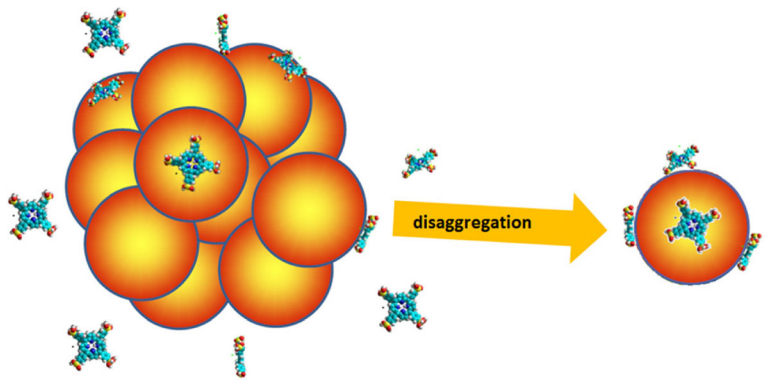

Scheme 1 The scheme of the interaction between aged (CdSe/ZnS)-Cys 558 QD and $TPPS_4$ porphyrin at neutral pH. The porphyrin molecules adsorb on the QD surface due to the high affinity of the porphyrin π-conjugated system for metal surfaces increasing the net negative charge on the QD surface, thus increasing electrostatic repulsion between particles and inducing their disaggregation

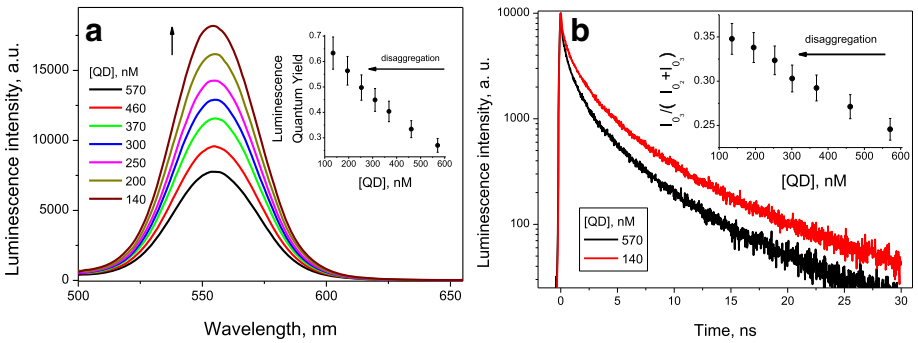

Fig. 4 **a** Luminescence spectra and quantum yield (inset) of aged (CdSe/ZnS)-Cys 558 QD solutions in function of its concentration. **b** Decay kinetics of the QD luminescence and the I_3 value (inset, see Eq. (3)) in function of its concentration

the solution storage (several months), etc. We plan to realize this profound study in the nearest future.

Conclusions

Basing on the obtained data, we can assert that the long storage of CdSe/ZnS-Cys QD in aqueous solutions even at low temperatures induces their aggregation, which reduces the luminescence quantum yield and lifetimes. The addition of $TPPS_4$ porphyrin stimulates disaggregation of aged CdSe/ZnS-Cys QD which is pronounced via increase of the QD luminescence quantum yield and the contribution of electron-hole annihilation in the QD shell in the total QD luminescence. The disaggregation, stimulated by porphyrin, takes place due to the increase of electrostatic repulsion between aggregated QD at their binding with negatively charged porphyrin molecules. Disaggregation has been observed at the dilution of QD solution, as well.

The obtained results demonstrate the way to repair the aged QD by adding some molecules or ions to solutions, stimulating QD disaggregation and restoring their luminescence characteristics, which could be important for QD biomedical applications, such as bioimaging and fluorescence diagnostics. On the other hand, disaggregation is important for QD applications in biology and medicine since it reduces the size of the particles facilitating their internalization into living cells across the cell membrane.

Additional file

Additional file 1: The experimental solutions were prepared in phosphate buffer (pH7.3;7.5mM), using Milli-Q quality water. **Figure S1**. Dynamic light scattering diagram of fresh prepared (CdSe/ZnS)-Cys 558 quantum dots (QD). **Figure S2**. Luminescence decay curve of freshly prepared (CdSe/ZnS)-Cys 558 QD solution; λ_{ex} =480nm and λ_{em} =558nm. **Figure S3**. **a** Normalized optical absorption spectrum of non-protonated $TPPS_4$. **Inset**: Normalized optical absorption spectra of the $TPPS_4$ Q-bands (black line) and "aged" QD (red line), and the fluorescence emission spectrum of non-protonated $TPPS_4$ with maximum at 644nm (blue line), λ_{ex} =515nm. **b** $TPPS_4$ fluorescence decay kinetics at 650nm, λ_{ex} =515nm. **Figure S4**. **a** Optical absorption spectra of the aged (CdSe/ZnS)-Cys 558 QD and $TPPS_4$ mixture at different $TPPS_4$ concentrations. **Inset**: Details of the absorption spectra in the region of the porphyrin Q-bands. **b** Optical absorption spectra just for $TPPS_4$ in the mixture $TPPS_4$ +QD. The final spectrum of each sample was obtained subtracting the initial QD absorption spectrum (no $TPPS_4$ adding). **c** Details of the absorption spectra in the region of the porphyrin Qbands, showing that $TPPS_4$ absorption spectrum does not change in the presence of aged (CdSe/ZnS)-Cys 558 QD. The curves for 0.1 and 0.3μM of $TPPS_4$ are not shown due to the lower signal-to-noise ratio of Qbands. No significant spectral shift was observed either Soret or Q-bands. **Figure S5**. **a** Normalized fluorescence excitation spectra of $TPPS_4$ in Milli-Q quality water as a function of $TPPS_4$ concentrations, λ_{em} =646nm. **b** Luminescence excitation spectra of $TPPS_4$ and aged (CdSe/ZnS)-Cys 558 QD mixtures as a function of $TPPS_4$ concentrations; λ_{em} =646nm; [QD]=570nM. **Figure S6**. **a** Zeta-potential measured on Malvern ZETASIZER 3000HSA (λ_{ex} =633nm, 10mW HeNe laser) **a** aged QD ($\xi_{aged\text{-}QD}$) and **b** $TPPS_4$ porphyrin (ξ_{TPPS4}). **Table S1**. Variation of aged (CdSe/ZnS)-Cys 558 QD hydrodynamic diameter (D_{hd}) as a function of its concentration measured on NanoBrook 90Plus Zeta Particle Size Analyzer (λ_{ex} =640nm, 40mW HeNe laser). (PDF 524 kb)

Abbreviations

C12-NBD-PC: 1-Palmitoyl,2-(12-[N-(7-nitrobenz-2-oxa-1,3-diazol-4-yl)amino]dodecanoyl)-sn-glycero-3-phosphocholine; FD: Fluorescence diagnostics; FP: Fluorescent probes; FWHM: Full width at half maximum; PCT: Photochemotherapy; PDT: Photodynamic therapy; PS: Photosensitizers; QD: Quantum dots; QD-Cys: Cysteine-coated QD; QY: Quantum yields; TOPO: Trioctylphosphine oxide; $TPPS_{44}$: *meso*-tetrakis (p-sulfonato-phenyl) porphyrin

Acknowledgements

The authors would like to thank Dr. Juliana C.B. Moraes from Departamento de Física e Química of Faculdade de Ciências Farmacêuticas de Ribeirão Preto –USP for her helpful suggestions.

Funding

The authors are indebted to São Paulo Research Foundation (FAPESP) by the grant #2011/20606-5, CNPq (Grant No. 305303/2013-9, Grant No. 309404/2015-0, and Grant No. 458436/2014-3), and Fundação de Amparo à Pesquisa do Estado de Goiás (FAPEG) Brazilian agencies and Russian Foundation for Basic Research (RFBR) (grant RFBR 15-29-01193) for partial financial support.

Authors' contributions

GGP and IEB conceived and designed the experiments. GGP and LPF carried out experiments in the presence of $TPPS_{44}$ porphyrin. GGP, LPF, PJG, and IEB analyzed the data and discussed the results. GGP, LPF, and IEB drafted the manuscript. SVS, VAO, VNM, and VAK synthesized and characterized the quantum dots. All authors have read and approved the final manuscript.

Ethics Approval and Consent to Participate
Not applicable

Consent for Publication
Not applicable

Competing Interests
The authors declare that they have no competing interests.

Publisher's Note

Author details
[1]Departamento de Física, Faculdade de Filosofia, Ciências e Letras de Ribeirão Preto, Universidade de São Paulo, Ribeirão Preto, SP 14040-901, Brazil. [2]Instituto de Física, Universidade Federal de Goiás, Caixa Postal 131, Goiânia, GO 74001-970, Brazil. [3]Shemyakin-Ovchinnikov Institute of Bioorganic Chemistry RAS, 16/10 Miklukho-Maklaya str, Moscow, Russia117997. [4]Emanuel Institute of Biophysical Chemistry, RAS-RU, Moscow, Russia. [5]Present Address: MackGraphe, Mackenzie Presbyterian University, São Paulo, SP 01302-907, Brazil.

Received: 1 August 2017 Accepted: 20 January 2018
Published online: 05 February 2018

References
1. Burda C, Chen X, Narayanan R, El-Sayed MA (2005) Chemistry and properties of nanocrystals of different shapes. Chem Rev 105:1025–1102. https://doi.org/10.1021/cr030063a
2. Michalet X (2005) Quantum dots for live cells, in vivo imaging, and diagnostics. Science (80-) 307:538–544. https://doi.org/10.1126/science.1104274
3. Loss D, DiVincenzo DP (2005) Quantum computation with quantum dots. Physics (College Park Md) 57:12. https://doi.org/10.1103/PhysRevA.57.120
4. Tong X, Zhou Y, Jin L et al (2017) Heavy metal-free, near-infrared colloidal quantum dots for efficient photoelectrochemical hydrogen generation. Nano Energy 31:441–449. https://doi.org/10.1016/j.nanoen.2016.11.053
5. Frasco MF, Chaniotakis N (2010) Bioconjugated quantum dots as fluorescent probes for bioanalytical applications. Anal Bioanal Chem 396:229–240. https://doi.org/10.1007/s00216-009-3033-0
6. Azzazy HME, Mansour MMH, Kazmierczak SC (2007) From diagnostics to therapy: prospects of quantum dots. Clin Biochem 40:917–927. https://doi.org/10.1016/j.clinbiochem.2007.05.018
7. Dayal S, Królicki R, Lou Y et al (2006) Femtosecond time-resolved energy transfer from CdSe nanoparticles to phthalocyanines. Appl Phys B Lasers Opt 84:309–315. https://doi.org/10.1007/s00340-006-2293-z
8. Karakoti AS, Shukla R, Shanker R, Singh S (2015) Surface functionalization of quantum dots for biological applications. Adv Colloid Interf Sci 215:28–45. https://doi.org/10.1016/j.cis.2014.11.004
9. Chen L-N, Wang J, Li W-T, Han H-Y (2012) Aqueous one-pot synthesis of bright and ultrasmall CdTe/CdS near-infrared-emitting quantum dots and their application for tumor targeting in vivo. Chem Commun 48:4971. https://doi.org/10.1039/c2cc31259j
10. Shibu ES, Hamada M, Murase N, Biju V (2013) Nanomaterials formulations for photothermal and photodynamic therapy of cancer. J Photochem Photobiol C Photochem Rev 15:53–72. https://doi.org/10.1016/j.jphotochemrev.2012.09.004
11. Gromova Y a, Orlova AO, Maslov VG et al (2013) Fluorescence energy transfer in quantum dot/azo dye complexes in polymer track membranes. Nanoscale Res Lett 8:452. https://doi.org/10.1186/1556-276X-8-452
12. Henglein A (1989) Small-particle research: physicochemical properties of extremely small colloidal metal and semiconductor particles. Chem Rev 89:1861–1873. https://doi.org/10.1021/cr00098a010
13. Liu W, Hak SC, Zimmer JP et al (2007) Compact cysteine-coated CdSe(ZnCdS) quantum dots for in vivo applications. J Am Chem Soc 129:14530–14531. https://doi.org/10.1021/ja073790m
14. Mroz P, Yaroslavsky A, Kharkwal GB, Hamblin MR (2011) Cell death pathways in photodynamic therapy of cancer. Cancers (Basel) 3:2516–2539. https://doi.org/10.3390/cancers3022516
15. Tita SPS, Perussi JR (2001) The effect of porphyrins on normal and transformed mouse cell lines in the presence of visible light. Brazilian J Med Biol Res 34:1331–1336. https://doi.org/10.1590/S0100-879X2001001000014
16. Borissevitch IE, Parra GG, Zagidullin VE et al (2013) Cooperative effects in CdSe/ZnS-PEGOH quantum dot luminescence quenching by a water soluble porphyrin. J Lumin 134:83–87. https://doi.org/10.1016/j.jlumin.2012.09.008
17. Liu J, Yang X, Wang K et al (2011) A switchable fluorescent quantum dot probe based on aggregation/disaggregation mechanismw. Chem Commun 47:935–937. https://doi.org/10.1039/c0cc03993d
18. Nabiev I, Sukhanova A, Even-Desrumeaux K et al (2012) Engineering of ultra-small diagnostic nanoprobes through oriented conjugation of single-domain antibodies and quantum dots. Protoc Exch:1–23. https://doi.org/10.1038/protex.2012.042
19. Aggarwal LPF, Borissevitch IE (2006) On the dynamics of the $TPPS_4$4 aggregation in aqueous solutions. Spectrochim Acta Part A Mol Biomol Spectrosc 63:227–233. https://doi.org/10.1016/j.saa.2005.05.009
20. Yu WW, Qu L, Guo W, Peng X (2003) Experimental determination of the extinction coefficient of CdTe, CdSe, and CdS nanocrystals. Chem Mater 15:2854–2860. https://doi.org/10.1021/cm034081k
21. Lakowicz JR (2006) Principles of fluorescence spectroscopy, 3rd ed. Springer, Boston
22. Chattopadhyay A (1990) Chemistry and biology of N-(7-nitrobenz-2-oxa-1,3-diazol-4-yl)-labeled lipids: fluorescent probes of biological and model membranes. Chem Phys Lipids 53:1–15. https://doi.org/10.1016/0009-3084(90)90128-E
23. Fery-Forgues S, Fayet J-P, Lopez A (1993) Drastic changes in the fluorescence properties of NBD probes with the polarity of the medium: involvement of a TICT state? J Photochem Photobiol A Chem 70:229–243. https://doi.org/10.1016/1010-6030(93)85048-D
24. Ji X, Peng F, Zhong Y et al (2014) Fluorescent quantum dots: synthesis, biomedical optical imaging, and biosafety assessment. Colloids Surfaces B Biointerfaces 124:132–139. https://doi.org/10.1016/j.colsurfb.2014.08.036
25. Xiao G, Wang Y, Ning J et al (2013) Recent advances in IV–VI semiconductor nanocrystals: synthesis, mechanism, and applications. RSC Adv 3:8104. https://doi.org/10.1039/c3ra23209c
26. Dahan M, Laurence T, Pinaud F et al (2001) Time-gated biological imaging by use of colloidal quantum dots. Opt Lett 26:825–827. https://doi.org/10.1364/OL.26.000825
27. Oleinikov V, Sukhanova A, Nabiev I (2007) Fluorescent semiconductor nanocrystals for biology and medicine. Nanotechnologies Russ 2:160–173
28. Wang Y, Herron N (1991) Nanometer-sized semiconductor clusters: materials synthesis, quantum size effects, and photophysical properties. J Phys Chem 95:525–532. https://doi.org/10.1021/j100155a009
29. Bawendi MG, Steigerwald ML, Brus LE (1990) The quantum mechanics of larger semiconductor clusters. Annu Rev Phys Chem 41:477–496. https://doi.org/10.1146/annurev.physchem.41.1.477
30. Brus L (1986) Electronic wave functions in semiconductor clusters: experiment and theory. J Phys Chem 90:2555–2560. https://doi.org/10.1021/j100403a003
31. Alejo T, Paulo PMR, Merchán MD et al (2017) Influence of 3D aggregation on the photoluminescence dynamics of CdSe quantum dot films. J Lumin 183:113–120. https://doi.org/10.1016/j.jlumin.2016.11.002
32. Martín-García B, Paulo PMR, Costa SMB, Velázquez MM (2013) Photoluminescence dynamics of CdSe QD/polymer Langmuir–Blodgett thin films: morphology effects. J Phys Chem C 117:14787–14795. https://doi.org/10.1021/jp311492z
33. Adeli M, Kalantari M, Sagvand M (2012) Hybrid nanomaterials consisting of pseudorotaxanes, pseudopolyrotaxanes, rotaxanes, polyrotaxanes, nanoparticles and quantum dots, p 30
34. Sui C, Liu Y, Li P et al (2013) Determination of IO4-and Ni2+ ions using L-cysteine-CdTe/ZnS quantum dots as pH-dependent fluorescent probes. Anal Methods 5:1695–1701. https://doi.org/10.1039/c3ay26426b
35. Kalyanasundaram K (1991) Photochemistry of polypyridine and porphyrin complexes. Academic Press, New York
36. Borissevitch IE, Tominaga TT, Imasato H, Tabak M (1996) Fluorescence and optical absorption study of interaction of two water soluble porphyrins with bovine serum albumin. The role of albumin and porphyrin aggregation. J Lumin 69:65–76. https://doi.org/10.1016/0022-2313(96)00037-3
37. Perrin ML, Prins F, Martin CA et al (2011) Influence of the chemical structure on the stability and conductance of porphyrin single-molecule junctions. Angew Chemie - Int Ed 50:11223–11226. https://doi.org/10.1002/anie.201104757

38. JKM S, Bampos N, Clyde-Watson ZE et al (2000) Inorganic, organometallic and coordination chemistry. In: Kadish KM, Smith KM, Guilard R (eds) The Porphyrin handbook, 1st edn. Academic Press, San Diego, pp 1–48
39. Zhang Y, Mi L, Wang PN et al (2008) pH-dependent aggregation and photoluminescence behavior of thiol-capped CdTe quantum dots in aqueous solutions. J Lumin 128:1948–1951. https://doi.org/10.1016/j.jlumin.2008.06.004
40. Rotomskis R, Augulis R, Snitka V et al (2004) Hierarchical structure of $TPPS_4$ 4 J-aggregates on substrate revealed by atomic force microscopy. J Phys Chem B 108:2833–2838. https://doi.org/10.1021/jp036128v
41. Magno LN, Bezerra FC, Freire LES et al (2017) Use of spectroscopic techniques for evaluating the coupling of porphyrins on biocompatible nanoparticles. A potential system for photodynamics, theranostics, and nanodrug delivery applications. J Phys Chem A 121:1924–1931. https://doi.org/10.1021/acs.jpca.6b10314
42. Shaikh AJ, Rabbani F, Sherazi TA et al (2015) Binding strength of porphyrin-gold nanoparticle hybrids based on number and type of linker moieties and a simple method to calculate inner filter effects of gold nanoparticles using fluorescence spectroscopy. J Phys Chem A 119:1108–1116. https://doi.org/10.1021/jp510924n